AD-A031 313 PANAMETRICS INC WALTHAM MASS F/G 4/1
AN ELECTROSTATIC ANALYZER FOR AN AIR FORCE SATELLITE PAYLOAD. E--ETC(U)
JUL 76 F A HANSER, B SELLERS F19628-73-C-0019

UNCLASSIFIED AFGL-TR-76-0203 NL

1 OF 1
ADA031313

END

DATE
FILMED
11 -76

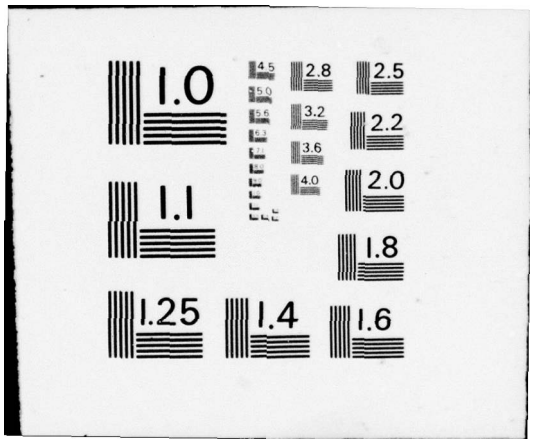
1.0
1.1
1.25
1.4
1.6
1.8
2.0
2.2
2.5
2.8
3.2
3.6
4.0
4.5
5.0
5.6

AFGL-TR-76-0203

AN ELECTROSTATIC ANALYZER FOR AN AIR FORCE SATELLITE PAYLOAD - EVALUATION OF IN-FLIGHT OPERATION

Frederick A. Hanser
Bach Sellers

Panametrics, Inc.
221 Crescent Street
Waltham, Massachusetts 02154

July 1976

Final Report
Period Covered - December 1972 to July 1976

AIR FORCE GEOPHYSICS LABORATORY
AIR FORCE SYSTEMS COMMAND
UNITED STATES AIR FORCE
HANSCOM AFB, MASSACHUSETTS 01731

Unclassified

SECURITY CLASSIFICATION OF THIS PAGE (When Data Entered)

(9) Final rept. Dec 72-Jul 76.

REPORT DOCUMENTATION PAGE

READ INSTRUCTIONS BEFORE COMPLETING FORM

1. REPORT NUMBER (18) (19) AFGL-TR-76-0203	2. GOVT ACCESSION NO. ✓
3. RECIPIENT'S CATALOG NUMBER	
4. TITLE (and Subtitle) (6) AN ELECTROSTATIC ANALYZER FOR AN AIR FORCE SATELLITE PAYLOAD - EVALUATION OF IN-FLIGHT OPERATION.	5. TYPE OF REPORT & PERIOD COVERED Final Report December 1972 to July 1976
	6. PERFORMING ORG. REPORT NUMBER
7. AUTHOR(s) (10) Frederick A. Hanser Bach Sellers	8. CONTRACT OR GRANT NUMBER(s) (15) F19628-73-C-0019 ✓
9. PERFORMING ORGANIZATION NAME AND ADDRESS PANAMETRICS, INC. 221 Crescent Street Waltham, Massachusetts 02154	10. PROGRAM ELEMENT, PROJECT, TASK AREA & WORK UNIT NUMBERS 76010901 62101F
11. CONTROLLING OFFICE NAME AND ADDRESS Air Force Geophysics Laboratory Hanscom AFB, Massachusetts 01731 Contract Monitor: Dr. R. P. Vancour/PHG	12. REPORT DATE (11) July 1976
	13. NUMBER OF PAGES 29 (12) 28 p.
14. MONITORING AGENCY NAME & ADDRESS (if different from Controlling Office) (16) AF-7601 (17) 760109	15. SECURITY CLASS. (of this report) Unclassified
	15a. DECLASSIFICATION/DOWNGRADING SCHEDULE

16. DISTRIBUTION STATEMENT (of this Report)

Approved for public release; distribution unlimited.

17. DISTRIBUTION STATEMENT (of the abstract entered in Block 20, if different from Report)

18. SUPPLEMENTARY NOTES

19. KEY WORDS (Continue on reverse side if necessary and identify by block number)

Electron Detector
Electrostatic Analyzer
Satellite Particle Detector

20. ABSTRACT (Continue on reverse side if necessary and identify by block number)

A satellite-borne electron spectrum analyzer has been developed, fabricated and flown on the S3-2 satellite. The instrument is a parallel plate electrostatic analyzer, and makes a 32-point spectrum analysis of electrons between 0.08 to 17 keV. The electron ESA was launched in late 1975, and was still operating properly in July 1976. Much electron data from the north and south auroral zones and polar regions has been returned. The ESA appears to be

(over)

DD FORM 1 JAN 73 1473 EDITION OF 1 NOV 65 IS OBSOLETE

Unclassified

SECURITY CLASSIFICATION OF THIS PAGE (When Data Entered)

403420

capable of operating properly for some years, assuming normal operation of the other satellite components.

FOREWORD

The research and construction reported herein were carried out under Contract No. F19628-73-C-0019. Special appreciation is given to the Air Force Geophysics Laboratory personnel whose cooperation helped to make the project successful, particularly to Dr. R. P. Vancour, the Contract Monitor, who provided technical guidance throughout the program and handled many of the details involved in integrating the instrument into the S3-2 satellite. The help of the personnel at the Air Force Satellite Control Facility in Sunnyvale, California, is also appreciated.

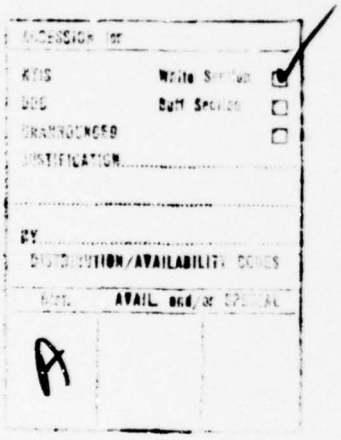

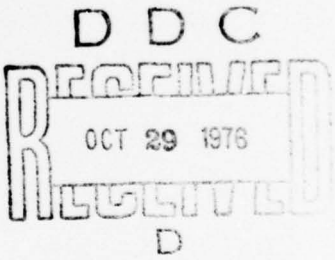

TABLE OF CONTENTS

LIST OF ILLUSTRATIONS

LIST OF TABLES

I. INTRODUCTION

The auroral zone and polar cap regions have various patterns of keV electron precipitation. In particular, auroral arcs are associated with intense, narrow bands of nearly monoenergetic electrons. While the keV electron precipitation patterns have been studied by rocket and satellite instrumentation for many years, the information on these patterns is by no means complete, and there is still much detail in the known precipitation patterns which can be profitably studied further.

An electrostatic analyzer (ESA) for electron detection was launched on the S3-2 satellite in late 1975. This ESA, one of two built for satellite use, was still operating properly in July 1976 and seems likely to operate reliably for a number of years, provided other satellite components allow it.

A parallel-plate electrostatic analyzer for electrons in the approximate range 1 to 20 keV was developed and fabricated by Panametrics, Inc., for use on rockets. Several of these ESA's had been successfully launched into auroral breakups at Ft. Churchill, Manitoba, Canada, and the basic design had thus been proven in actual use. The rocket payload design for the ESA made use of the comparatively high power levels and telemetry rates available from rockets, and was therefore not an optimum design for satellite use. The basic instrument design was thus modified to minimize weight and power requirements, and the data output put into a form suitable for a satellite telemetry system. The final instrument was designed to be compatible with integration into an Air Force satellite payload, and to make use of the allotted telemetry.

The satellite parallel-plate ESA design detects electrons over the approximate range 0.08 to 17 keV in 32 energy bins. A complete spectrum is swept out in about 1 second, with alternate sweeps being from high to low, and low to high, energy. Each energy bin is sampled twice in succession, with only the accumulated counts being sent to telemetry. Thus, the unit gives 64 count samples per second. The basic design is discussed in detail in Refs. 1.1 and 1.2.

The following sections present first a summary description of the flight ESA, and then a discussion of the first turn-on operation and normal orbital operation. The final section presents conclusions and recommendations with regard to the instrument design and applications of the data. An outline of the ESA data analysis procedure is given in the Appendix.

II. SUMMARY DESCRIPTION OF THE FLIGHT ESA

A detailed description of the two satellite ESA's (flight and back-up units) constructed has been given in Ref. 1.1. Basically, the instrument is a parallel plate ESA for measuring electrons in the .08 to 17 keV range. The flight unit was launched in late 1975 and was still operating properly in July 1976. A summary of the satellite ESA characteristics is given in Table 2.1. The electron energies detected are listed in Table 2.2. The summing bin widths are needed to calculate the total electron flux and energy flux (see Appendix). The electron spectrum is swept once every second, with each energy bin being counted twice for a nominal 1/64 second. Successive sweeps are from channel 00 to 37 (octal) and from 37 to 00, so a complete instrument cycle takes a nominal two seconds. Ten analog monitors are used to check proper ESA operation, with monitored functions as given in Table 2.3.

The basic analysis of a parallel plate ESA has been given in Refs. 2.1, 2.2, and 2.3, with a short summary of the flux calculation equations in Ref. 1.1. The basic equations are repeated in the Appendix, which contains an outline of the data analysis procedure.

Table 2.1

Summary of Flight ESA Characteristics

Particles Detected:	Electrons
Detector:	Channeltron Electron Multiplier
Method of Energy Analysis:	Electrostatic Deflection
Energy Range:	0.08 to 17 keV
Energy Bins:	32 (see Table 2.2)
Geometric Factor:	4.68×10^{-5} cm^2 - sr
Counting Accuracy:	Statistical
In-Flight Calibration Means:	Co^{57} and Electronic Test Pulse Generator
Size:	320 cu. in.
Weight:	7.5 lbs
Power Requirements:	28 ± 4 VDC, 3.0 W
Number of Analog Outputs:	10 (see Table 2.3)
Analog Output Signal Level:	0 to 5 Volts
Analog Output Source Impedance:	5 kΩ
Digital Output Format:	16 Bits Serial

Table 2.2

Data on the Electron Energy Steps for the Flight ESA

Decimal Code	Octal Code	Plate voltage (kV)	Electron energy (keV)	Summing bin width (keV)
0	00	0.049	0.082	0.022
1	01	0.062	0.104	0.031
2	02	0.086	0.144	0.051
3	03	0.122	0.205	0.071
4	04	0.171	0.287	0.097
5	05	0.237	0.398	0.138
6	06	0.336	0.564	0.197
7	07	0.472	0.792	0.269
8	10	0.656	1.101	0.386
9	11	0.932	1.564	0.549
10	12	1.311	2.200	0.472
11	13	1.494	2.507	0.277
12	14	1.641	2.754	0.275
13	15	1.822	3.057	0.282
14	16	1.978	3.319	0.317
15	17	2.20	3.69	0.375
16	20	2.42	4.06	0.39
17	21	2.67	4.48	0.44
18	22	2.94	4.93	0.47
19	23	3.23	5.42	0.51
20	24	3.55	5.96	0.57
21	25	3.91	6.56	0.60
22	26	4.26	7.15	0.65
23	27	4.69	7.87	0.74
24	30	5.14	8.62	0.82
25	31	5.67	9.51	0.91
26	32	6.23	10.45	0.99
27	33	6.84	11.48	1.12
28	34	7.57	12.70	1.23
29	35	8.30	13.93	1.32
30	36	9.14	15.34	1.47
31	37	10.06	16.88	1.54

Table 2. 3

Analog Monitors for ESA

Number	Function Monitored
1	+ 10V
2	+ 15V
3	- 5V
4	+ 10V REFERENCE
5	+ 28V
6	Temperature
7	+ 3kV
8	+ 3kV Input Current
9	- 10kV Input Current
10	- 10kV Reference Input

III. IN-FLIGHT OPERATION OF THE ESA

The flight ESA was launched as part of the payload of the S3-2 satellite late in 1975. Initial turn-on occurred a few days after launch, which allowed sufficient time for payload outgassing to avoid corona problems with the high voltages. The ESA was still operating properly in July 1976.

III. 1 First Turn-on Operation

The first turn-on of the satellite ESA is critical in that it must be turned off promptly should any malfunction occur. The two high voltage supplies are the important components to watch. Should gas pressure from outgassing components be large enough to cause breakdown, then the high voltage supplies could be destroyed if left on for too long. Any corona that occurs can damage the channel multiplier (CM) electron detector, primarily by causing severe gain loss in the CM. Thus during first ESA turn-on, the high voltage monitors (see Table 2. 3) are watched, and the ESA turned off at any sign of non-normal operation.

The first turn-on occurred a few days after launch, and no problems were encountered. All monitors were giving proper values, and the counts from the CM were as expected for non-auroral conditions. Should there have been any problems, it was planned to leave the ESA off for another day for further outgassing and then try turn-on again.

For the next few days the ESA was turned on several times during auroral zone passes in an attempt to observe auroral electrons. One successful pass was made through the northern night auroral zone on December 8, 1975. Some weak electron fluxes were detected during a portion of this pass. The counts from four consecutive scans (4 seconds) were summed and the electron spectrum calculated. The spectrum is plotted in Fig. 3. 1, along with the more intense flux observed on March 26, 1976 (see next section). Since the satellite spin period was about 8 seconds the spectrum in Fig. 3. 1 is an average over all pitch angles, and over about 30 km across the auroral zone (the satellite velocity is about 7. 5 km/sec).

The electron spectrum in Fig. 3. 1 shows peaks at 2. 5 keV and 12 keV. Considering the large spatial and pitch angle average, this is a reasonable auroral electron spectrum. It shows that the ESA is operating properly and is detecting electrons as it was designed to do. The initial turn-on of the satellite ESA was accomplished with no problems.

III. 2 Normal Orbital Operation

The electron ESA on satellite S3-2 was launched in late 1975, and normal satellite operation started in December 1975. The satellite is in a near polar orbit with about 1 deg per day precession of the orbital plane, so it remains near the noon-midnight meridian throughout the year. Design lifetime of the satellite is six months, so with proper ESA operation in July 1976 the instrument has performed better than required. Generally, about two orbits of data per day have been acquired.

The large amount of data received from the ESA makes it desirable to have some preliminary data plots to help locate the most important data more quickly. Such plots have been provided in the form of 64 count sums over two consecutive channels, vs time, for each half orbit. Since each channel has two counts per second, this yields one point for each 16 seconds, and a total of 32 plots per orbit, all on microfiche. Typical examples of these plots are shown for March 26, 1976, during a magnetically active period, in Figs. 3. 2 and 3. 3. The counts are plotted on a logarythmic scale, with GMT, latitude, invariant latitude, and altitude given on the bottom scale.

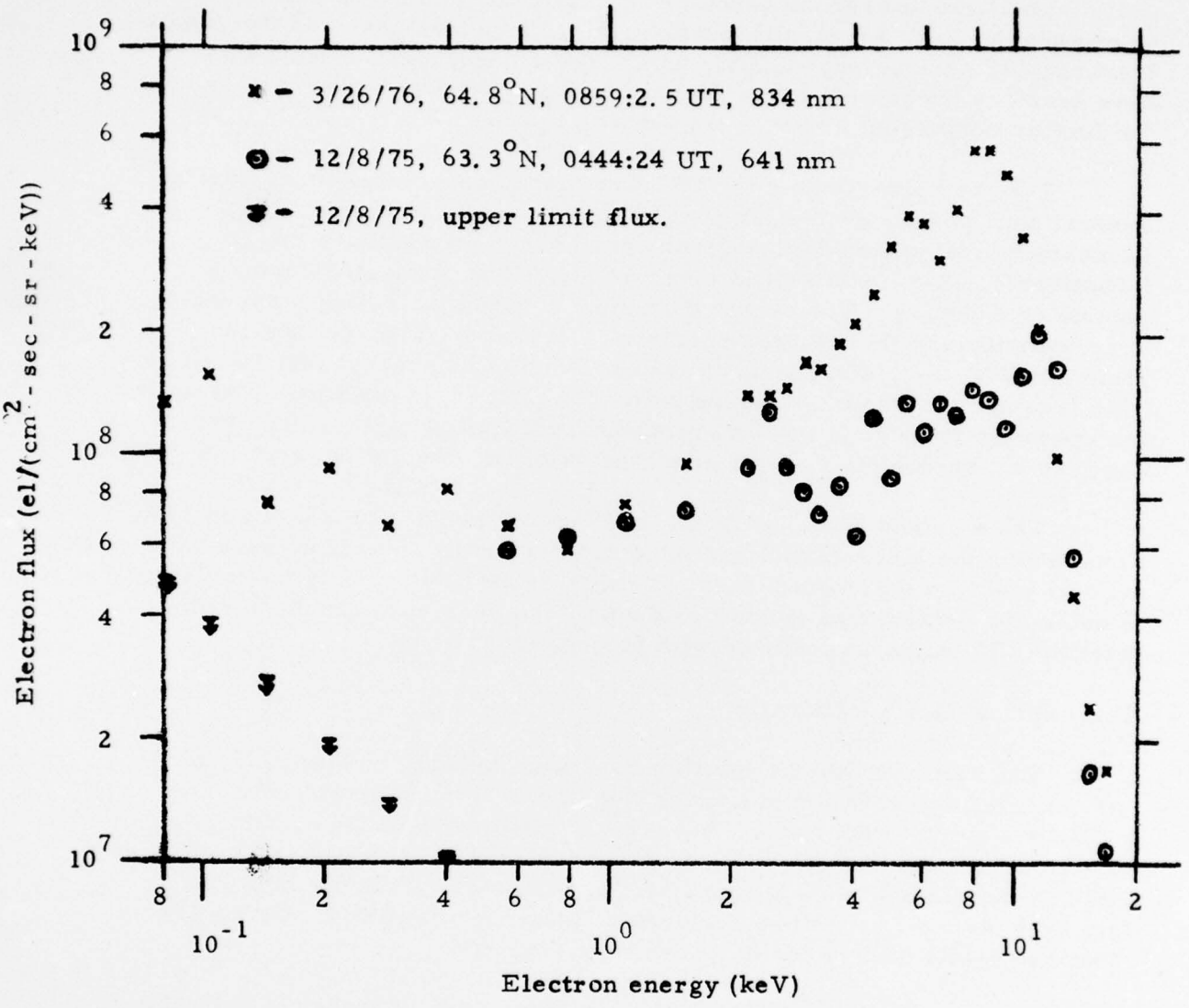

Fig. 3.1. Electron Spectra Measured on December 8, 1975, and March 26, 1976 by ESA on S3-2.

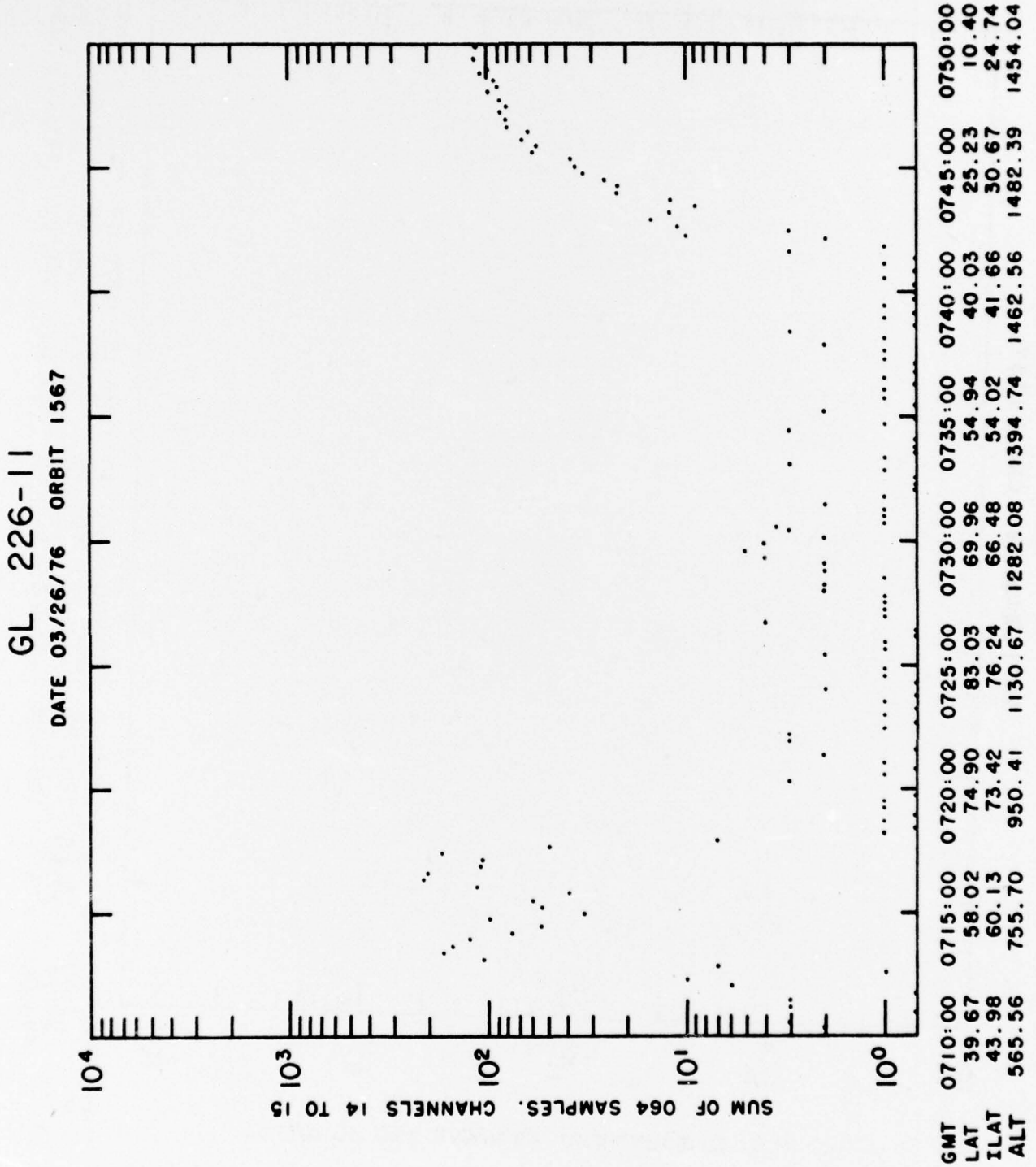

Fig. 3.2. Plot of 64 Count Sums for ESA Channels 14 and 15, for a North Pole Pass on March 26, 1976.

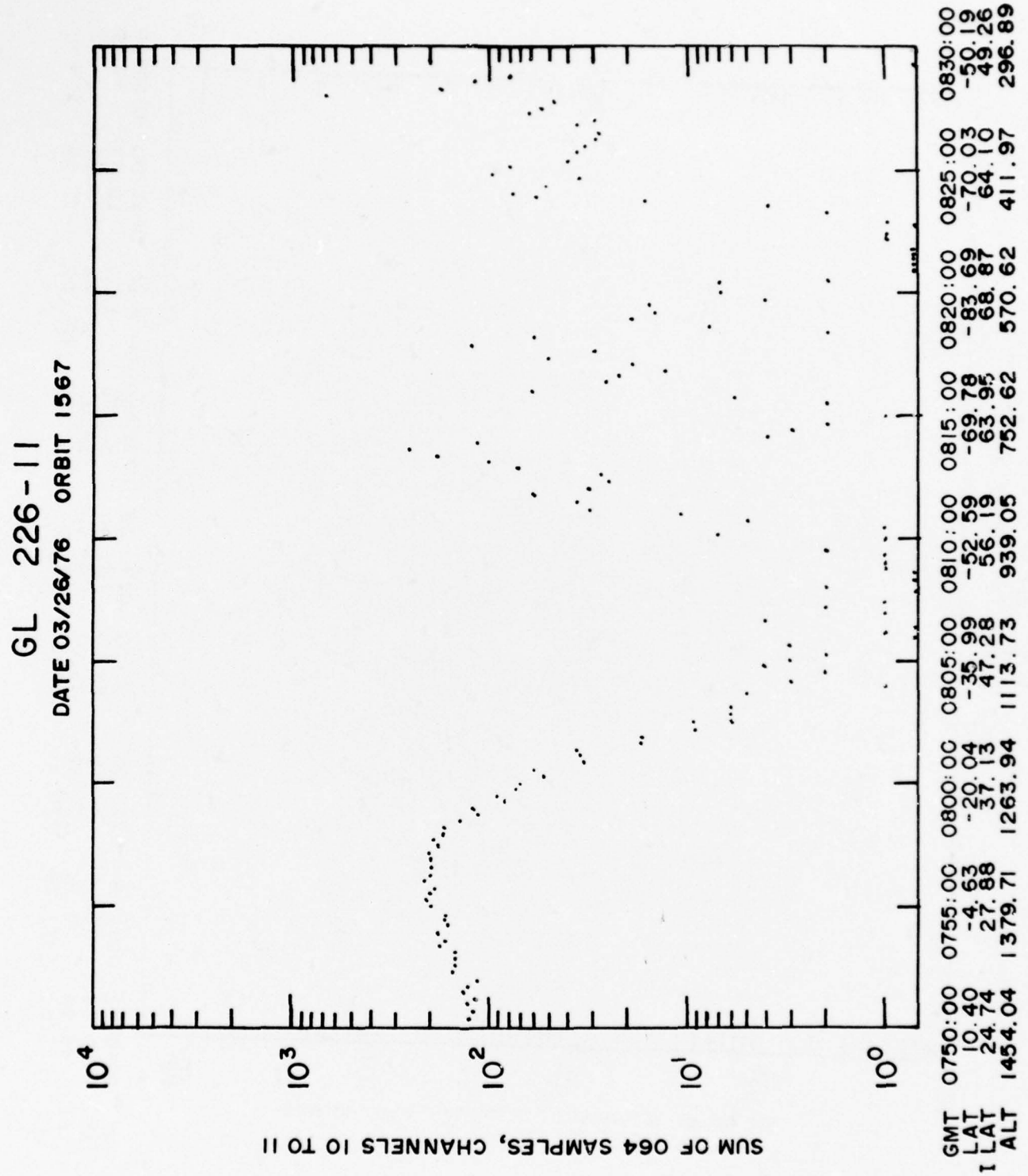

Fig. 3.3. Plot of 64 Count Sums for ESA Channels 10 and 11, for a South Pole Pass on March 26, 1976.

Figure 3.2 shows a strong electron flux in the night-side auroral zone, and a weak flux in the day-side. The rise in counts south of about 35^{o}N latitude is background from penetrating protons in the inner radiation belt. The second part of this orbit (1567) is shown in Fig. 3.3 for ESA channels 10 and 11. North of latitude 35^{o}S the radiation belt background is seen, and then two bands of electrons on the day-side of the pole. The most intense, third, band of electrons is seen in the night-side auroral zone. The fluxes in Figs. 3.2 and 3.3 are among the most intense measured by the electron ESA on S3-2, and are associated with the strong magnetic activity of March 26-27.

The spin period of S3-2 is about 20 seconds, so a one second spectrum covers about 18^{o} of rotation. The detailed count print-out for the March 26-27 data shows the pitch angle distribution of the electrons as a 20-sec periodicity in the counts. Since the satellite velocity is about 7.5 km/sec, one complete satellite rotation covers about 150 km in horizontal distance. During the March 26-27 event the ESA measured peak count rates in excess of 10^{4}/sec, which is still well within the capability of the CM electron detector. Such count rates are achieved only a fraction of the time, so the 10^{10}- 10^{11} count life of the CM before gain degradation should not be reached for some years. Thus this ESA design is also suitable for longer-life satellites, even when it is expected to be on continuously.

A reduced electron spectrum from orbit 1568 on March 26 is shown in Fig. 3.1. This spectrum is for precipitated electrons in the northern, night-side auroral zone. The spectrum is an average over 6 seconds of data (12-1/64 sec counts), covering about 108^{o} of satellite rotation and 45 km in horizontal travel. The spectrum shows a strong peak near 8 keV, and possibly a secondary peak at 5-6 keV. From the individual 1 sec count sequences it is obvious that there is some spatial and pitch angle variation in the fluxes, so the spectrum in Fig. 3.1 is an average, not an instantaneous electron spectrum. The spectrum is, however, reasonably consistent with the measured auroral electron spectra (see Ref. 2.2, e.g.).

The March 26, 1976 electron spectrum can be readily compared with the December 8, 1975 spectrum also plotted in Fig. 3.1. Both show a sharp decline in the flux above 15 keV. The greater flux in the 3-10 keV region is obvious, although the 0.5-3 keV region does not appear to be significantly different. Below 0.5 keV the December 8 data gave no counts, so the only comparison can be made with the (1σ) upper limit flux, which appears to be lower.

The electron ESA operation in orbit appears to be as expected. No monitor voltages have been observed to deviate significantly from before-launch ground check values, and the measured, reduced electron spectra appear to be valid. An outline of the ESA data analysis procedure is given in the Appendix. The ESA has operated properly for in excess of six months, the minimum required lifetime, and appears quite likely to operate reliably for much longer, other satellite systems permitting.

IV. CONCLUSIONS AND RECOMMENDATIONS

IV. 1 Summary of In-Flight Operation

The electron ESA on S3-2 was launched in late 1975, and has operated reliably for more than the required minimum of six months. Returned electron data give high quality spectra and show the ESA is operating properly. Since only one ESA unit is on board, pitch-angle information can only be obtained through satellite spin at the rate of 1 rotation/20 secs. However, the energy spectrum is scanned once per second with much higher resolution than is normal for satellite spectrometers. An outline of the analysis procedure is given in the Appendix.

During the one second required for the ESA to measure a full electron spectrum the satellite moves about 7.5 km across the auroral zone. Since the satellite spin period is about 20 seconds, a complete pitch angle scan, made in one-half rotation, covers about 75 km across the auroral zone. Auroral forms are frequently much less than 75 km, so the satellite ESA makes only crude measurements of the electron pitch angle distribution associated with such forms. Certain types of auroral events, for example the 'inverted-V', may be up to several hundred km across (see Sec. IV. 2 below). For such events this ESA can provide extremely useful information, with much better energy resolution than has previously been possible from satellites. In events of this type the pitch-angle distribution is particularly important, however, as it is for investigation of luminous auroral forms. For future satellites it would thus be desirable to have several of these high energy resolution ESA's on board to improve the pitch angle coverage.

The back-up ESA was originally scheduled to undergo long-term vacuum tests at the AFGL. These tests were never made, and are probably now unnecessary, since the flight unit has proven itself in the vacuum of near-earth space. From the operation of the flight ESA to date, it is likely that this type satellite ESA unit would operate reliably in space for a number of years, with the major limitation being the operation of other satellite components.

The geometric factor and energy resolution of the parallel plate ESA can be quite readily calculated (Ref. 2.3). The detection efficiency of the channel multiplier (CM) is more difficult to determine. The electron detection efficiency given in the Appendix is calculated from the measurements of Ref. 4.1, and is used as the best available. It is well known, however, that CM detection efficiency depends on the precise type and can vary appreciably from one type to the next. Should it later be possible to measure the actual detection efficiency of the back-up ESA, these measured results would be better for use in the ESA data analysis. Use of such a measured efficiency function in the analysis would be quite straightforward, since the necessary count data are available in the data base defined at the beginning of the Appendix.

Operation of the flight ESA can thus be summarized:

i) Initial turn-on showed no problems, with the ESA operating properly from the start.

ii) The ESA has operated properly for in excess of the required six months, and it should operate properly for some time should the other satellite components allow it.

iii) The quality of the high resolution electron spectra measured by the ESA appears to be quite good. Much data from the north and south polar regions have been returned.

Recommendations with regard to the ESA itself can be summarized as follows:

i) For future satellites it would be desirable to have more than one ESA on board to improve electron pitch angle coverage in narrow auroral forms.

ii) The CM electron detection efficiency should be measured in the back-up unit to improve the accuracy of the detection efficiency used in the data analysis.

IV.2 Data Applications

Since the S3-2 ESA requires about 20 seconds to complete a pitch-angle scan (via satellite rotation), it is principally suited to measurement of auroral events in which the pitch angle distribution is relatively constant over distances greater than 50 km or so. A highly resolved energy spectrum can be determined once per second, however, hence the energy-dependence of such a constant pitch angle distribution can be measured

very accurately. Optimum application of the S3-2 ESA will thus be to those types of auroral events that are relatively stable in time (tens of seconds) and in which the uniquely good energy resolution of the device will be an advantage.

Much useful data of a general survey, or statistical occurrence basis, can of course be generated to supplement and improve that already in existence. For example, to determine the average spectral characteristics at various locations with better resolution than previously possible. Recent summaries of previous survey data have been made by Hultqvist (Ref.4.2) and Frank et al.(Pef.4.3). The latitudinal morphology of 10eV to 10keV electrons as determined from Isis 1 and 2 has been reported by Winningham et al.(Ref.4.4) and by Torr and Torr (Ref. 4.5) in the 0.2 to 26keV region as measured from the AEC satellite. A general survey of polar cap fluxes determined from Isis 1 is given by Winningham and Heikkila (Ref. 4.22). The 2 to 500eV AEC data are discussed by Doering et al. (Ref. 4.6). Data in the 0.2 to 12keV region as measured from Ariel 4 are reported by Craven and Frank (Refs. 4.7 and 4.8).

Interestingly, in 1975 Boyd commented (Ref.4.9) that "monoenergetic peaks" similar to those observed in intense arcs by Westerlund (Ref.4.10) had not been observed from a satellite. One of the possible explanations given was that the previous satellite instruments did not have sufficient energy resolution (Ref. 4.9, p. 739). In fact, some of the Ariel 4 satellite spectra given by Craven and Frank in 1975 (Ref.4.7) show clear peaks in the energy spectrum near 1 keV. The S3-2 ESA, which has even better resolution that that on Ariel 4, has also observed such peaks as shown, for example, by the two peaks in Fig. 3.1. Energy spectra reported by Mizera et al.(Ref.4.11) as measured on the S72-1 satellite also show such peaks. Thus, "monoenergetic peaks" can definitely be observed from satellites, provided the instrument resolution is sufficiently good.

It is generally believed that such peaks in the electron spectrum are caused by electric fields aligned along the magnetic field direction (see Ref. 4.12 for various pertinent references). One of the manifestations of such an effect is called the 'inverted-V' (IV) event, so-called because as the event is traversed by a satellite the average energy is found to increase to a peak - in the region of maximum electric field - and subsequently decrease (Ref. 4.8). Near the region of maximum field intensity the electron pitch angle distribution can be highly field aligned. Such events may be hundreds of km in extent (Ref. 4.8), although they may be considerably narrower. Figure 4.1 shows the energy of the principal spectral peak (which is related to the average spectral energy) for the March 26, 1976 northern auroral zone pass, as measured by the S3-2 ESA. This is a good example of an IV event some 50-75 km wide.

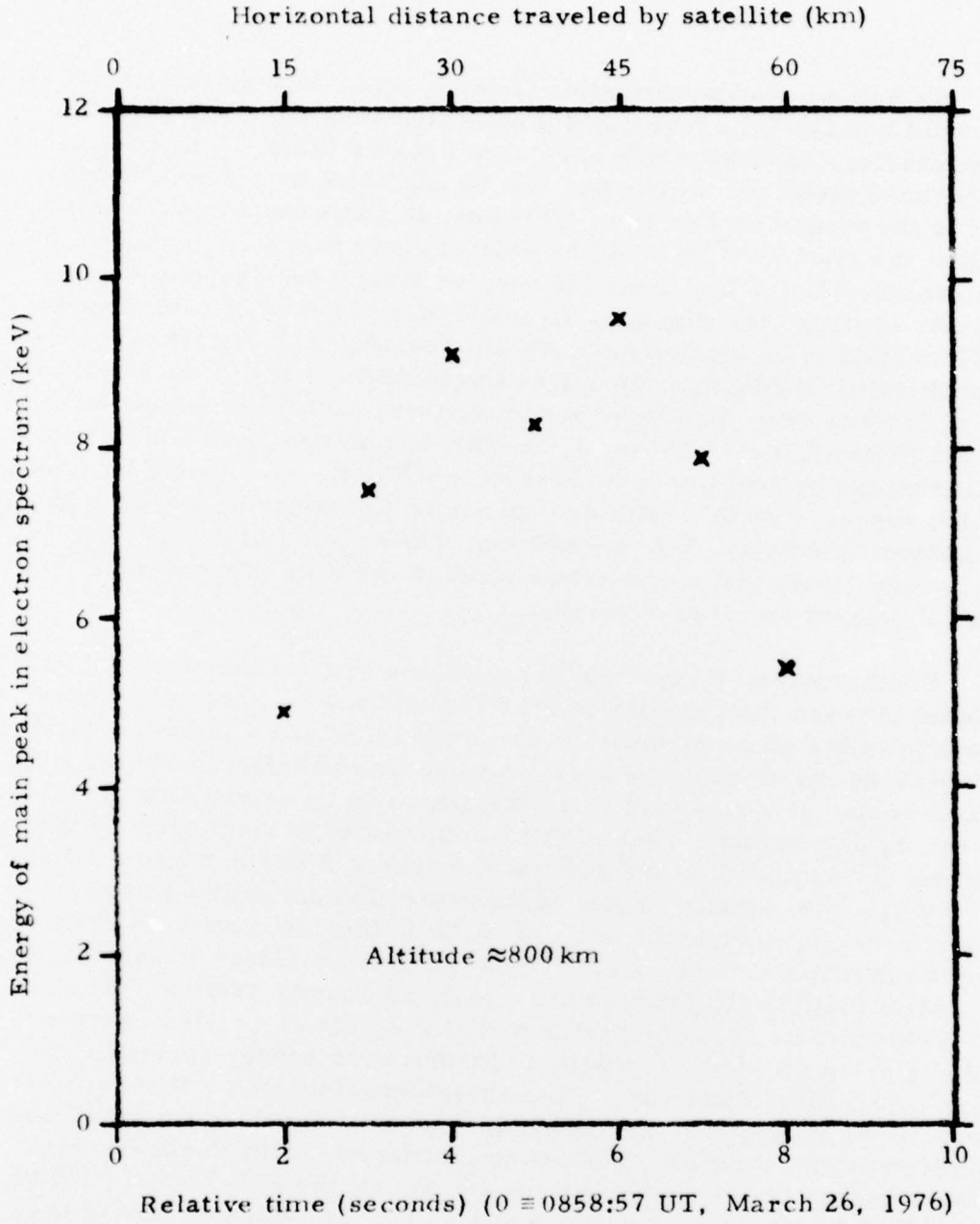

Fig. 4.1. Variation of Peak in Electron Spectrum for March 26, 1976 Northern Auroral Zone Pass.

We believe that investigation of the spectral characteristics of IV events could be one of the more useful applications of the S3-2 ESA data. Previous studies, some of which have used rockets (Refs. 4.13, 4.14, 4.15), have measured electron spectra that can be explained by electric fields parallel to the magnetic field (Ref. 4.11) and, in some instances, it is suggested that the electric field could be located close to the ionosphere. In a basic investigation of the effects of such an E field on electron energy and angular spectra, for example, Evans (Ref. 4.16) in 1974 considered a 1 kV/100km field to be located near 200 km altitude. In a statistical study of the probability of finding field-aligned precipitation at a fixed electron energy of 2. 3 keV (assumed to be associated with E field acceleration) Berko and Hoffman (Ref. 4.17) used satellite data at two pitch angles to conclude that the probability is highest near ~800 km. Comments by Evans (Ref. 4.18) suggest that this altitude depends on the electron energy. Since the maximum altitude of S3-2 is ~1500 km, while the minimum is near 240 km, it is very likely that a statistical study of the ESA spectra would provide useful data on inverted-V events.

Furthermore, it also appears probable that a significant E field could exist between the satellite and the atmosphere - say the 100 km level. If it were possible simultaneously to measure the spectra in both locations during an IV event, it would be possible to prove the existence of the field in a given region of space, and much insight could be gained into the mechanism for its production. That such a simultaneous measurement might be carried out is suggested by the work of Vondrak and Baron (Refs. 4.19 and 4.20). By use of e-density versus altitude profiles determined by the Chatanika radar (geomagnetic latitude 64.75°), they developed an unfolding method to determine the electron energy spectrum incident on the atmosphere that is required to produce the measured density profile. Thus, if such a measurement could be performed at the time of an S3-2 overpass, it would be possible to obtain a set of simultaneous energy spectra measured at two distinct points on a single magnetic field line. If enough such sets were to be measured, it is likely that an inverted-V event would be encountered in that location. Following discussions with Vondrak, such a series of measurements was carried out during the Feb-March 1976 period. Vondrak (private communication, 4/1/76) has indicated that of this series, those of immediate interest (based on ground-based observations in the vicinity of Chatanika) are as follows:

Chatanika Satellite Overpass

Time(UT)			Alt.
Day	Hr	Min	km
46	07	35	316.7
47	07	28	308.9
53	08	28	249.8
63	07	08	273.0

During the entire initial series of measurements the satellite altitude did not exceed 500 km on an overpass. Those listed above are even lower and would serve principally to verify the energy spectrum determination method developed by Vondrak (assuming that the satellite spectra show interesting structure). This, in itself, is a very useful objective. Of course, a significant E field could have been encountered on one of these passes, but it is more probable that such fields would be observed for higher altitude overpasses.

Clearly, the data reduction procedure described in the Appendix should be applied to the above overpasses to determine the energy and, to the extent possible, the angular spectra in the vicinity of Chatanika. Additional coordinated measurements should be made, if possible, emphasizing higher altitude passes. In addition to the original work of Evans (Ref. 4.16) on the effect of ionospheric E fields on electron energy and angular spectra, additional work has been done taking into account the effects of rapidly time-varying fields (Ref. 4.21) and detector energy resolution (Ref. 4.15). All of these effects would have to be taken into account in comparing the atmospheric electron spectrum with that measured at the satellite, provided an E field is encountered. Furthermore, in the presence of such a field the pitch angle distribution is generally anisotropic, being highly field-aligned. The effects of such a deviation from isotropy on the measured e-density profile would have to be considered.

In conclusion, with regard to the S3-2 ESA electron data, we recommend the following:

i) The data base should be examined on a statistical basis for augmentation of previous survey data.

ii) The high energy resolution capability of the device should be utilized to examine the details of energy spectra and its dependence on altitude, latitude, etc., during inverted-V events.

iii) The Chatanika overpasses should be examined in detail, as described above, and additional coordinated measurements should be carried out, if possible.

REFERENCES

1.1 P. R. Morel, F. A. Hanser and B. Sellers, Design, Fabrication, and Integration of An Electrostatic Analyzer for a Satellite Payload, Scientific Report No. 1, AFCRL-TR-75-0017 (December 1974). AD A006698

1.2 P. R. Morel, F. A. Hanser, and B. Sellers, An Electrostatic Analyzer for an Air Force Satellite Payload, Scientific Report No. 2, AFCRL-TR-75-0366 (July 1975). AD A015798

2.1 B. Sellers, F. A. Hanser, and J. L. Hunerwadel, Research in the Design, Development and Construction of Non-magnetic Sensors for Magnetic Field-Charged Particle Correlation Studies, Final Report, AFCRL-68-0585 (Oct. 1968). AD 681454

2.2 F. A. Hanser, B. Sellers, and P. R. Morel, Design and Flight of Charged Particle Detection Systems for Rocket Experiments, Final Report, AFCRL-71-0484 (August 1971). AD 736417

2.3 F. A. Hanser, B. Sellers, and J. L. Hunerwadel, Design and Flight Evaluation of Charged Particle Detection Systems for Rocket Experiments, Final Report, AFCRL-TR-73-0612 (August 1973). AD772735

4.1 R. J. Archuleta and S. E. DeForest, Efficiency of Channel Electron Multipliers for Electrons of 1-50 keV, Rev. Sci. Instr., 42, 89-91 (1971).

4.2 B. Hultqvist, Rocket and Satellite Observations of Energetic Particle Precipitation in Relation to Optical Aurora, Ann. Geophys. 30, 223-57 (1974).

4.3 L. A. Frank, N. A. Saflekos, and K. L. Ackerson, Electron Precipitation in the Postmidnight Sector of the Auroral Zones, J. Geophys. Res. 81, 155-67 (1976).

4.4 J. D. Winningham, F. Yasuhara, S-I. Akasofu, and W. J. Heikkila, The Latitudinal Morphology of 10-eV to 10-keV Electron Fluxes During Magnetically Quiet and Disturbed Times in the 2100-0300 MLT Sector, J. Geophys. Res. 80, 3148-71 (1975).

4.5 D. G. Torr, M. R. Torr, R. A. Hoffman and J. C. G. Walker, Global Characteristics of 0.2 to 26 keV Charged Particles at F Region Altitudes, Geophys. Res. Lett. 3, 305-8 (1976).

REFERENCES (cont'd)

4.6 J. P. Doering, W. K. Peterson, C. O. Bostrom, and J. C. Armstrong, Measurement of Low-Energy Electrons in the Day Airglow and Day Side Auroral Zone from Atmosphere Explorer C, J. Geophys. Res. 80, 3934-44 (1975).

4.7 J. D. Craven and L. A. Frank, Observations of Angular Distributions of Low Energy Electron Intensities over the Auroral Zones with Ariel 4, Proc. R. Soc. Lond. A. 343,167-88 (1975).

4.8 J. D. Craven and L. A. Frank, Electron Angular Distributions Above the Day Side Auroral Oval, J. Geophys. Res. 81, 1695-9 (1976).

4.9 J. S. Boyd, Rocket-Borne Measurements of Auroral Electrons, Rev. Geophys. and Space Phys. 13,735-40 (1975).

4.10 L. H. Westerlund, The Auroral Electron Energy Spectrum Extended to 45eV, J. Geophys. Res. 74,351-4 (1969).

4.11 P. F. Mizera, D. R. Croley, Jr., and J. F. Fennell, Electron Pitch-angle Distributions in an Inverted 'V' Structure, Geophys. Res. Lett. 3, 149-52 (1976).

4.12 R. L. Arnoldy, R. A. Hendrickson and J. R. Winckler, Echo 2: Observations at Fort Churchill of a 4-keV Peak in Low-Level Electron Precipitation, J. Geophys. Res. 80, 2316-18 (1975).

4.13 A. D. Johnstone and T. N. Davis, Low-Altitude Acceleration of Auroral Electrons During Breakup Observed by a Mother-Daughter Rocket, J. Geophys. Res. 79, 4616-25 (1974).

4.14 J. M. Bosqued, G. Cardona and H. Rème, Auroral Electron Fluxes Parallel to the Geomagnetic Field Lines, J. Geophys. Res. 79, 98-104 (1974).

4.15 R. Lundin, Rocket Observations of Electron Spectral and Angular Characteristics in an "Inverted V" Event. Planet. Space Sci. 24, 499-514 (1976).

4.16 D. S. Evans, Precipitating Electron Fluxes Formed by a Magnetic Field Aligned Potential Difference, J. Geophys. Res. 79, 2853-8. (1974).

4.17 F. W. Berko and R. A. Hoffman, Dependence of Field-Aligned Electron Precipitation Occurrence on Season and Altitude, J. Geophys. Res., 79, 3749-54 (1974).

4.18 D. S. Evans, Comment on 'Dependence of Field-Aligned Electron Precipitation Occurrence on Season and Altitude' by F. W. Berko and R. A. Hoffman, J. Geophys. Res., 81, 3425-6 (1976).

4.19 R. R. Vondrak, The Energy Distribution of Incident Auroral Electrons as Determined from Ground-Based Radar Measurements, Paper SA61, Dec. 8-12, 1975 American Geophys. Union, San Francisco, Calif. (1975).

4.20 R. R. Vondrak and M. J. Baron, A Method of Obtaining the Energy Distribution of Auroral Electrons from Incoherent-Scatter Radar Measurements, in Proceedings of EISCAT Summer School, Tromso, Norway (1975).

4.21 D. S. Hall and D. A. Bryant, Energy and Angular Distribution of Auroral Particles Resulting from Time-Varying Acceleration in ESRO Special Publication SP-107 (1975).

4.22 J. D. Winningham and W. J. Heikkila, Polar Cap Auroral Electron Fluxes Observed with Isis 1, J. Geophys. Res. 79, 949-57 (1974).

APPENDIX

OUTLINE OF ANALYSIS PROCEDURE FOR SATELLITE ELECTRON ESA DATA

The raw satellite ESA data consist of the two sets of 32 energy bin counts accumulated during each complete cycle (2 x 32 = 64 per second) and the necessary auxiliary data required during analysis. As a minimum these auxiliary data should allow ready calculation, for each ESA count if necessary, of the following parameters: GMT (or UT), altitude, longitude, geocentric latitude, geomagnetic latitude, invariant latitude, magnetic field, L-shell, local time, magnetic local time, and magnetic pitch angle of the detected electrons. From this data base for each orbit, the following analysis procedure applies.

ESA data: 32 energy bins - E_i, i = 1, 32
Each bin has an energy width ΔE_i
2 counts at each step - nominal 1 sec cycle.

The energy bin values, E_i, and widths for summing, ΔE_i, are given in Table 2.2 (Note - Table 2.2 uses i = 0, ---, 31, whereas here i = 1, ---, 32 in decimal).

The analysis then proceeds as follows:

1) Select data to analyze (use only 1 of 4 possible modes):

   a) Only use 1st of each double count.

   b) Only use 2nd of each double count.

   c) Do each count, but separately (may be two separate runs in a) and b)).

   d) Do all counts, no distinction.

2) Read in latitude range for this orbit, and latitude intervals for summing:

   a) Read Lat (start), Lat (finish). When the range goes over one of the poles the bin where the maximum latitude is achieved should be noted. The bin where sun/dark transition takes place should also be noted. (Note: normally invariant latitude will be used, but the option to use geocentric latitude should be retained.)

b) Read Lat (decrement) mode (use either i) or ii)):

i) Use Δ Lat, going from Lat (start) to Lat (start) + Δ Lat, + 2 Δ Lat, etc. to Lat (finish).

ii) Or, read in N Lat breakpoints, go from Lat (start) to Lat (1), Lat (1) to Lat (2), --- to Lat (finish).

3) Read in pitch angle ranges to use (either a) or b)):

a) Read Δ PA, go from PA (min) (normally = 0^{o}) to PA (max) (normally = 180^{o}) in steps of Δ PA.

b) Read in NPA breakpoints, PA(j), and go from PA(j) to PA(j + 1), etc.

4) Read in energy bin ranges to use (either a) or b)):

a) SUM N_E consecutive bins (N_E = 1 is no sum, and may be used); i.e., go from (1---N_E), (N_E + 1---2N_E), (nN_E + 1---32). Note that last bin may not be N_E wide!

b) Read N'_E breakpoints, $N_E''(j)$. Sums are from $N_E''(1)$-$N_E''(2)$, $N_E''(2)$ + 1 - $N_E''(3)$, etc.

5) Read in the Plotting methods (may do only one, any two, or all three):

a) Plot energy spectrum for each PA bin. Plot will be $\bar{J}$ (flux) vs log $\bar{E}$ (energy). For each latitude interval the mode of plotting is (either i) or ii)):

i) All PA bins are on one plot (points, but no error bars).

ii) Only one PA bin per plot, but with error bars shown for each point. Note that the log $\bar{E}$ scale is fixed, but the log $\bar{J}$ scale may vary from run to run.

b) Plot the PA distribution for each latitude interval. Mode of plotting is (either i) or ii)):

i) All energy bins on one plot (points but no error bars).

ii) Only one energy bin per plot, but with error bars shown for each point. Note: the PA scale is linear (usually 0^{o} to 180^{o}), but the flux scale can be either $\bar{J}$ or log $\bar{J}$, as selected by input data.

c) Plot a latitude distribution for each PA/E bin. The plots will be log $\overline{J}$ vs latitude, with GMT, local time, altitude, and possibly other data, printed under the latitude. Plots will be made in one of the following modes:

1) Do all points at each latitude.
2) For each PA bin, plot all energy points at each latitude. (This gives PA bin # plots.)
3) For each energy bin, plot all PA points at each latitude. (This gives E bin # plots.)
4) Make a separate latitude plot for each PA/E bin, plotting both points and error bars.

The above plots should generally be done on a CRT, with the option to use a paper plotter if desired.

Equations for ESA analysis:

There are 32 energy bins to start - with energy E(i) and effective width $\Delta E(i)$ given as fixed parameters (can use DATA statement). The values for E(i) and $\Delta E(i)$ are given in Table 2.2.

If the individual counts for bin i are $M_j(E_i)$, then the average count is

$$M(E_i) = \sum_{j=1}^{J} M_j(E_i)/J \qquad \text{(A.1)}$$

The flux in bin i is then given by

$$j_m(E_i) = \frac{M(E_i)/\Delta T}{G\,\epsilon(E_i')\,f_r\,E_i} \qquad \text{(A.2)}$$

where $\Delta T \simeq 1/64$ sec (may be corrected if actual cycle time is not 1 sec), $G = 4.68 \times 10^{-5}$ cm^2-sr, $f_r = 0.0419$, and

$$\epsilon(E_i') = 1 - \left[\frac{2}{3 + \frac{6.5}{(E_i' - 0.5)} + \frac{30}{(E_i' - 0.5)^3}}\right] \qquad \text{(A.3)}$$

with $E_i' = E_i + 0.1$, and $\epsilon(E_i') = 1.0$ if $E_i' \leq 0.5$. An alternative to calculating

$\epsilon(E_i')$ as above is to use a table (32 entries). This may be necessary if calibration shows that the actual $\epsilon(E_i')$ differ from the analytical fit (A. 3).

The statistical error in the flux is

$$\delta j_m(E_i) = j_m(E_i) \Big/ \sqrt{\sum M_j(E_i)} \quad , \text{ if } \sqrt{\quad} > 0 \qquad \text{(A. 4a)}$$

$$= (0.5/\Delta T)/(G\,\epsilon(E_i')\,f_r\,E_i) \quad , \text{ if } \sqrt{\quad} = 0 \text{ and } J > 0 \qquad \text{(A. 4b)}$$

$$= 0 \quad , \text{ if } J = 0 \qquad \text{(A. 4c)}$$

The fluxes for plotting are calculated as follows:

6) First sort into pitch angle bins for each energy, and calculate fluxes as above, $j_m(E_i) \pm \delta j_m(E_i)$, (32 fluxes for each PA range).

7) Sum over energy bins, as follows:

$$\bar{J}\,(\bar{E}) = \sum_{i=j_1}^{j_2} j_m(E_i)\,\Delta E_i \Big/ \sum_i \Delta E_i \qquad \text{(A. 5)}$$

$$\overline{\delta J}\,(\bar{E}) = \left[\sum_{i=j_1}^{j_2} (\delta j_m(E_i)\Delta E_i)^2\right]^{1/2} \Big/ \sum_i \Delta E_i \qquad \text{(A. 6)}$$

$$\bar{E} = \sum_{i=j_1}^{j_2} E_i/(j_2 - j_1 + 1) \qquad \text{(A. 7)}$$

The values of j_1 and j_2 are the breakpoint indices from 4) above. Note that the sums are $j_1 \text{---} j_2$, $j_2 + 1 \text{---} j_3$, etc., to avoid using the breakpoint bin in two flux averages.

For each pitch angle bin calculate the average energy, total energy flux, and total flux, from

$$E_{av} = \frac{\sum_{i=1}^{32} j_m(E_i)\,\Delta E_i\,E_i}{\sum_{i=1}^{32} j_m(E_i)\,\Delta E_i} \qquad \text{(A. 8)}$$

$$J_{E\,tot} = \sum_{i=1}^{32} j_m(E_i)\,\Delta E_i\,E_i \qquad \text{(A. 9)}$$

and

$$J_{tot} = \sum_{i=1}^{32} j_m(E_i)\,\Delta E_i \qquad \text{(A. 10)}$$

The final outputs are:

8) For each latitude interval:

   a) Print out the averaged flux spectrum for each PA bin and the averages caculated above. This includes the $\overline{J}$, $\overline{\delta J}$, and $\overline{E}$ from (A. 5), (A. 6), and (A. 7) for each PA bin, and the overall averages E_{av}, $J_{E\,tot}$, and J_{tot} from (A. 8), (A. 9), and (A. 10).

   b) Make plots, as necessary (input data determine which plots are to be done, if any).

9) At end make latitude flux plots, as necessary.

   Note that steps 6), 7) and 8) must be repeated for each latitude interval, before step 9) is done at the end.

At some time in the future it may be desirable to add the fluxes from several orbits together to make synoptic plots covering long time periods. Thus an option should be included to output the $\overline{J}$, $\overline{\delta J}$ and $\overline{E}$, along with necessary identifying information, onto tape (or elsewhere) for storage and later summing.